

A space-time finite element method for neural field equations with transmission delays

Mónika Polner

Bolyai Institute, University of Szeged

Miklós Farkas Seminar on Applied Analysis, October 26, 2017



Joint work with Jaap van der Vegt & Stephan van Gils
University of Twente, The Netherlands

[P., van der Vegt, van Gils, SISC 2017]

“The work of M. Polner was supported by the János Bolyai Research
Scholarship of the Hungarian Academy of Sciences”



Outline

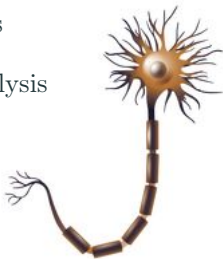
Biological inspiration

The mathematical model

Time-discontinuous Galerkin method for NF

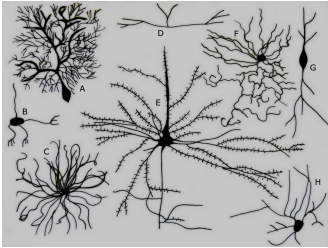
Numerical examples

Nonlinear error analysis

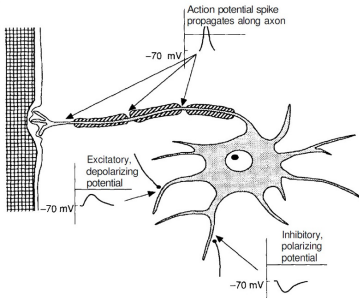


Biological inspiration

Biological inspiration



Neuron types



Connections, synapses,
action potential

A neural field model

Neural activity dynamics in a bounded, open, connected domain $\Omega \subset \mathbb{R}^d$, $d = 1, 2, 3$ is modeled by

$$\frac{\partial V_i}{\partial t}(t, r) = -\alpha_i V_i(t, r) + \sum_{j=1}^P \int_{\Omega} J_{ij}(r, r') S_j(V_j(t - \tau_{ij}(r, r'), r')) d r'.$$

$V_i(t, r)$ **membrane potential**

$J_{ij}(r, r')$ the **connectivity kernel**

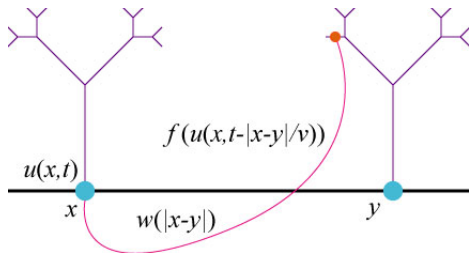
S_j the **synaptic activation function**

$\tau_{ij}(r, r')$ the **propagation delays**

[Wilson and Cowan, 1972; Amari, 1977]

A neural field model

$$\frac{\partial}{\partial t} u(t, x) = -\alpha u(t, x) + \underbrace{\int_{\Omega} w(x, y) f(u(t - \tau(x, y), y)) dy}_{\text{synaptic input}}$$



$$\tau(x, y) = \frac{|x - y|}{v}.$$

Delays in neural systems

Sources of delay:

- Due to propagation of action potentials along the axon and/or dendrite
- Due to the transmission of electric signals across the synapse

Play an important role in the spatiotemporal dynamics of neural activity.

The mathematical model

Neural field models as dynamical systems

The membrane potentials evolve according to the integro-differential equation with space dependent delay

$$\frac{\partial u}{\partial t}(t, \mathbf{x}) = -\alpha u(t, \mathbf{x}) + \int_{\Omega} J(\mathbf{x}, \mathbf{r}) S(u(t - \tau(\mathbf{x}, \mathbf{r}), \mathbf{r})) d\mathbf{r}$$

H_J The **connectivity kernel** $J \in C(\bar{\Omega} \times \bar{\Omega})$.

H_S The **synaptic activation function** $S \in C^\infty(\mathbb{R})$ and its k th derivative is bounded for every $k \in \mathbb{N}_0$.

H_τ The **delay function** $\tau \in C(\bar{\Omega} \times \bar{\Omega})$ is non-negative and not identically zero.

[S.A. van Gils e.a., 2013]

Choice of the State Space

$$\frac{\partial u}{\partial t}(t, x) = -\alpha u(t, x) + \int_{\Omega} J(x, r) S(u(t - \tau(x, r), r)) dr$$

The maximal delay

$$0 < \tau_{max} := \sup\{\tau(\mathbf{r}, \mathbf{r}') : \mathbf{r}, \mathbf{r}' \in \bar{\Omega}\} < \infty$$

Introduce $Y := C(\bar{\Omega})$, $X := C([- \tau_{max}, 0]; Y)$

Define the nonlinear operator $G : X \rightarrow Y$ (integral part that involves the history) by

$$G(\phi)(\mathbf{r}) := \int_{\Omega} J(\mathbf{r}, \mathbf{r}') S(\phi(-\tau(\mathbf{r}, \mathbf{r}'), \mathbf{r}')) d\mathbf{r}' \quad \forall \phi \in X, \forall \mathbf{r} \in \bar{\Omega}$$

Define the **history** at time $t \geq 0$ by

$$X \ni u_t(\theta) := u(t + \theta) \quad \forall t \geq 0, \theta \in [-\tau_{max}, 0]$$

Then studying of the neural field equation is equivalent to analyzing the following **Delay Differential Equation**:

$$\begin{cases} \dot{u}(t) = -\alpha u(t) + G(u_t) & t \geq 0 \\ u(t) = \phi(t) & t \in [-\tau_{max}, 0] \end{cases} \quad (\text{DDE})$$

where the solution $u \in C([-\tau_{max}, \infty); Y) \cap C^1([0, \infty); Y)$.

The state of the system at time $t \geq 0$

$$u_t(s)(x) = u(t + s, x), \quad s \in [-\tau_{max}, 0], x \in \Omega$$

The operator G is globally Lipschitz continuous.

Time-discontinuous Galerkin method for NF

Numerical study of NF

Difficulties: localized nature is lost (weight kernel), space-dependent time delays

First choice: approximations of NF with large systems of DDEs, the state space $C([- \tau_{max}, 0], Y)$ reduces to $C([- \tau_{max}, 0], \mathbb{R}^{m+1})$ (works well for special types of connectivity kernels)

[Faye and Faugeras, 2010]

New scheme: includes a convolution structure, hence allows fast numerical algorithms (works only for special types of connectivity kernels)

[Hutt and Rougier, 2014]

Our choice: Time-discontinuous (dGcG) finite element method

[P., van der Vegt, van Gils, SISC 2017]

Motivation of using dGcG method for NF

- The use of a space-time discretization is a natural way to deal with the space-dependent delays
- Well established to solve PDEs and stiff ODE systems
- It is well suited for mesh adaptation
- It has good long-time accuracy
- No restrictions to the functions involved in the system

The variational formulation:

Find $u \in C^1([0, T], Y) \cap C([- \tau_{max}, T], Y)$, such that

$$\begin{aligned}(\dot{u}(t) + \alpha u(t), v) - (G(u_t), v) &= 0, & \forall v \in Y, \forall t \in (0, T), \\ u(s) &= u^0(s), & s \in [-\tau_{max}, 0],\end{aligned}$$

where (\cdot, \cdot) is the $L^2(\Omega)$ inner product. The delay contribution is expressed as

$$(G(u_t), v) = \int_{\Omega} G(u_t)(x) v(x) dx$$

The space-time dGcG-FEM discretization

- $\mathcal{E} \subset \mathbb{R}^{d+1}$: open, bounded space-time domain in which a point has coordinates $(t, \mathbf{x}) \in \mathbb{R}^{d+1}$
- Partition the time interval $\bar{I} = [0, T]$ using the time levels $0 = t_0 < t_1 < \dots < t_N = T$, and denote by $I_n = (t_{n-1}, t_n]$ the n th time interval of length $k_n = t_n - t_{n-1}$
- A space-time slab is defined as $\mathcal{E}^n = I_n \times \Omega$

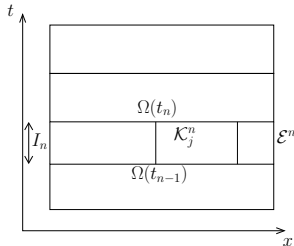


Figure 1: Two-dimensional space-time elements in physical space.

The space-time dGcG-FEM discretization

- Approximate the spatial domain Ω with Ω_h using a tessellation of non-overlapping hexahedral elements

$$\bar{\mathcal{T}}_h = \left\{ \mathcal{K}_j : \bigcup_{j=1}^M \bar{\mathcal{K}}_j = \bar{\Omega}_h, \mathcal{K}_j \cap \mathcal{K}_i = \emptyset \text{ if } i \neq j \right\}.$$

$\Omega_h \rightarrow \Omega$ as $h \rightarrow 0$,

- The space-time elements are obtained as $\mathcal{K}_j^n = (t_{n-1}, t_n) \times \mathcal{K}_j$.

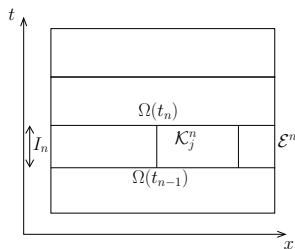


Figure 2: Two-dimensional space-time elements in physical space.

The *finite element space* associated with the tessellation \mathcal{T}_h^n is defined as:

$$V_h^n = \{u \in C^0(\mathcal{E}^n) : u|_{\mathcal{K}} \circ G_{\mathcal{K}}^n \in \left(\hat{\mathcal{P}}_q(-1,1) \otimes \hat{\mathcal{P}}_r(\hat{K})\right), \forall \mathcal{K} \in \mathcal{T}_h^n\}$$

The *weak formulation*: find $u_h \in V_h$ such that the variational equation holds for all $v \in V_h = \{u \in L^2(\mathcal{E}) : u|_{\mathcal{E}_n} \in V_h^n, n = 1, 2, \dots, N\}$.

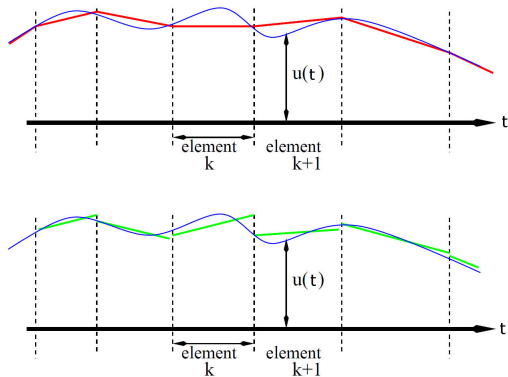


Figure 3: Continuous Galerkin FEM, where $u = u(t)$ is approximated globally in a (piecewise linear) continuous manner (top figure). In contrast, in a discontinuous Galerkin FEM, $u = u(t)$ is approximated globally in a discontinuous manner and locally in each element in a (piecewise linear) continuous way (bottom figure).

$$\dot{u}(t) = -\alpha u(t) + G(u_t), \quad G(\varphi)(x) = \int_{\Omega} J(x, r) S(\varphi(-\tau(x, r), r)) dr$$

The space-time dGcG-FEM method: find $u_h \in V_h$ such that

$$\sum_{n=1}^N \left[\sum_{\mathcal{K} \in \mathcal{T}_h^n} \left(\frac{\partial}{\partial t} u_h + \alpha u_h, v_h \right)_{\mathcal{K}} - \int_{I_n} \left(\hat{G}(u_{ht}), v_h(t) \right) dt \right]$$

$$+ \underbrace{\sum_{n=2}^N ([u_h]_{n-1}, v_h^{n-1,+}) + (u_h^{0,+}, v_h^{0,+})}_{\text{jump term}} = (u^0(0), v_h^{0,+})$$

holds for all $v_h \in V_h$

Here $[u_h]_n = u_h^{n,+} - u_h^{n,-}$, $u_h^{n,\pm} = \lim_{s \rightarrow 0^+} u_h(t_n \pm s, \cdot)$.

Finite element approximation

Introduce the approximation

$$u_h(t, x) |_{\mathcal{K}} = \sum_{m=1}^{N_p} \hat{u}_m^{\mathcal{K}} \psi_m^{\mathcal{K}}(t, x)$$

and set the test function $v_h(t, x) = \psi_i^{\mathcal{K}}(t, x)$, with $\psi_i^{\mathcal{K}}$ the Lagrange basis functions.

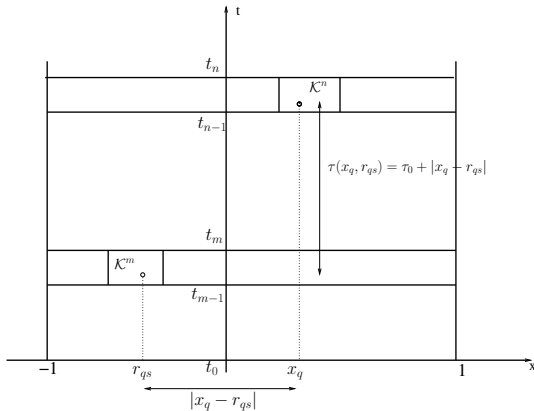
The delay term:

$$\begin{aligned} & \int_{\mathcal{K}} \psi_i^{\mathcal{K}}(t, x) \left(\int_{\Omega} J(x, r) S(u_h(t - \tau(x, r), r)) dr \right) dx dt \\ &= \int_{\mathcal{K}} \psi_i^{\mathcal{K}}(t, x) \left(\sum_{L \in \bar{\mathcal{T}}_h} \int_L J(x, r) S \left(\sum_{m=1}^{N_p} \hat{u}_m^L \psi_m^L(t - \tau(x, r), r) \right) dr \right) d\mathcal{K} \end{aligned}$$

How to treat the delay term?

$$\int_{\mathcal{K}} \psi_i^{\mathcal{K}}(t, x) \left(\sum_{L \in \tilde{\mathcal{T}}_h} \int_L J(x, r) S \left(\sum_{m=1}^{N_p} \hat{u}_m^L \psi_m^L(t - \tau(x, r), r) \right) dr \right) d\mathcal{K}$$

Fix a quadrature point $(t_q, x_q) \in \mathcal{K}^n$ in a space-time element. To compute the integral over a space element L , consider $r_{qs} \in \Omega$, and distinguish three cases for the time delay $t_q - \tau(x_q, r_{qs})$.



Numerical examples

Neural fields in 1D

Space and time are re-scaled such that $\bar{\Omega} = [-1, 1]$ and the propagation speed is 1,

$$\tau(x, r) = \tau_0 + |x - r|.$$

$$\frac{\partial u}{\partial t}(t, x) = -\alpha u(t, x) + \int_{-1}^1 J(x, r) S(u(t - \tau(x, r), r)) dr.$$

The connectivity and activation functions are, respectively,

$$J(x, y) = \hat{J}(|x - y|) = \sum_{j=1}^2 c_j e^{-\mu_j |x - y|}, \quad c_j \in \mathbb{R}, \mu_j \in \mathbb{R},$$

$$S(u) = \frac{1}{1 + e^{-\sigma u}} - \frac{1}{2}, \quad \forall u \in \mathbb{R}.$$

[S.A. van Gils e.a., 2013]

Characteristic equation

$$\frac{\partial u}{\partial t}(t, x) = -\alpha u(t, x) + \int_{\Omega} J(x, r) S'(0) u(t - \tau(x, r, r)) dr$$

$$\Delta(\lambda)q = 0, \quad q \in Y,$$

where $\Delta(\lambda) : Y \rightarrow Y$ is defined as

$$\Delta(\lambda)q = (\lambda + \alpha)q - e^{-\tau_0 \lambda} \sum_{i=1}^2 c_i K_i(\lambda)q,$$

$$c_i = \hat{c}_i \underbrace{S'(0)}_{=\sigma}, \quad k_i(\lambda) = \lambda + \mu_i,$$

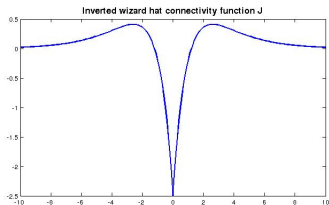
with $K_i(\lambda) : Y \rightarrow Y$

$$(K_i(\lambda)q)(r) = \int_{\Omega} e^{-k_i(\lambda)|r-r'|} q(r') dr'.$$

Neural field simulations

Hopf bifurcation

α	τ_0	σ	c_1	c_2	μ_1	μ_2
1.0	1.0	4.2202	3.0	-5.5	0.5	1



$$\hat{J}(x) = \hat{c}_1 e^{-\mu_1|x|} + \hat{c}_2 e^{-\mu_2|x|}, \quad |x| \leq 1,$$

The initial function for this simulation is $u(t, x) = \epsilon = 0.01$.

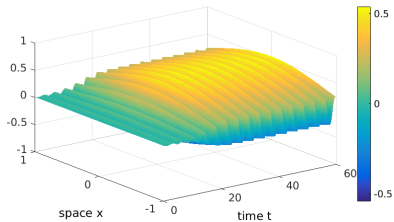
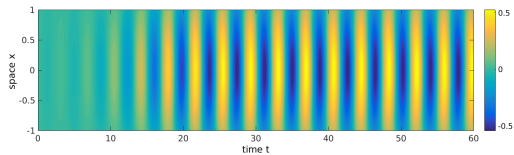


Figure 4: Time simulation of the system for $\sigma = 6$, beyond a Hopf bifurcation.

New simulations (adding spatial inhomogeneity)

Locally changed connectivity $\tilde{J}(x, y) = J(x, y) + \omega J(x, y) |_{\Omega_k}$

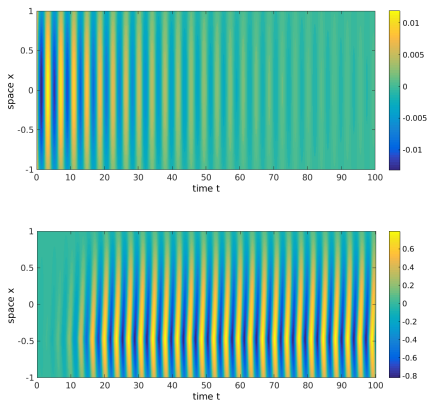
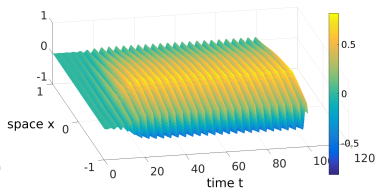
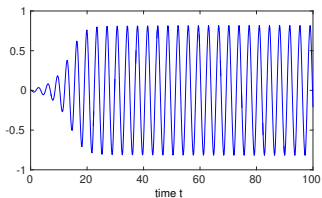
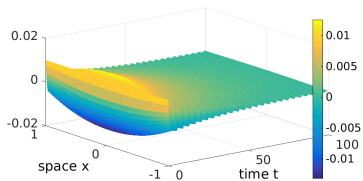
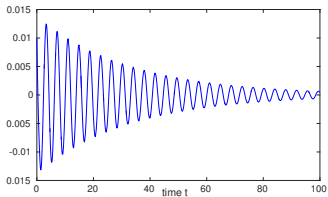


Figure 5: Time simulation of the system for $\sigma = 4$, in the homogeneous (top) and the inhomogeneous (bottom, $\omega = 15$) case.

Effect of spatial inhomogeneity



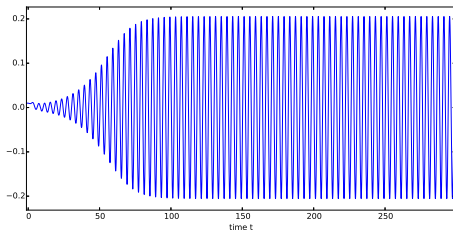
Neural fields in two space dimensions

$$\frac{\partial u}{\partial t}(t, x) = -\alpha u(t, x) + \int_{\Omega} J(x, r) S(u(t - \tau(x, r), r)) dr$$

First the connectivity function

$$J(x, r) = \hat{J}(\|x - r\|) = \hat{c}_1 e^{-\mu_1 \|x - r\|_1} + \hat{c}_2 e^{-\mu_2 \|x - r\|_1}, \quad x, r \in [-1, 1]^2$$

- For $\sigma = 4$ we obtain convergence to zero steady state.
- For $\sigma = 6$ we obtain periodic solution



Time-periodic solution, homogeneous kernel

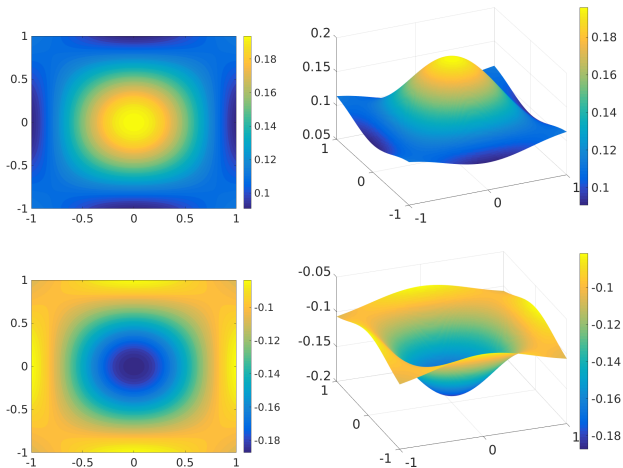


Figure 6: The solution of the system when $\sigma = 6$, at the beginning and at half of a time period.

Time-periodic solution, inhomogeneous kernel

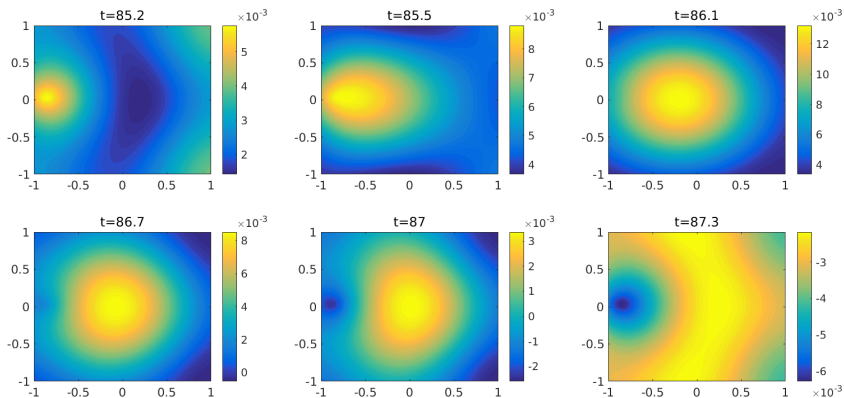


Figure 7: Time evolution of the system when $\sigma = 4$, during half of a time period, $\omega = 30$.

Neural fields in two space dimensions

Second example the connectivity kernel is defined as

$$J(x, r) = \hat{J}(\|x - r\|) = \frac{1}{\sqrt{2\pi\xi_1^2}} e^{-\frac{\|x-r\|^2}{2\xi_1^2}} - \frac{1}{\sqrt{2\pi\xi_2^2}} e^{-\frac{\|x-r\|^2}{2\xi_2^2}},$$

with $\xi_1 = 0.3$, $\xi_2 = 0.4$, the norm is the $\|\cdot\|_1$, $\sigma = 45$. The rate of natural decay of activity as bifurcation parameter, $\alpha = 1/5$.

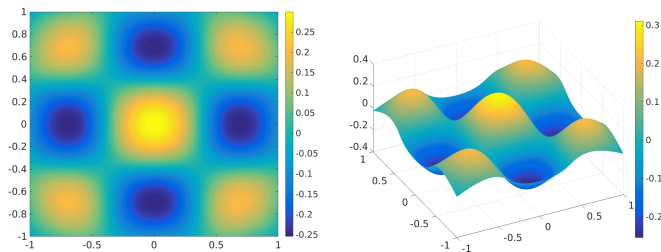


Figure 8: Pattern emerging in the two-dimensional neural field model with homogeneous connectivity and $\|\cdot\|_1$ -norm.

Neural fields in two space dimensions

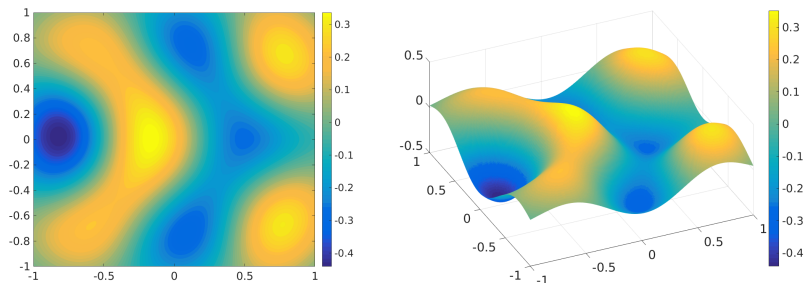


Figure 9: Pattern emerging in the two-dimensional neural field model with inhomogeneous connectivity, $\omega = 15$, and $\| \cdot \|_2$ -norm.

Error analysis

Theorem

Let $u \in C^1([0, T]; Y) \cap H^{q+1}([0, T]; H^{r+1}(\Omega))$ be the solution of the NF equation for some $q, r \geq 0$, with initial state $u_0 \in X \cap H^{q+1}([-\tau_{max}, 0]; H^{r+1}(\Omega))$, and let $u_h \in V_h^n$ be the dGcG solution. Then

$$\|u_h(t_N) - u(t_N)\|^2 \leq C \left(\sum_{i=1}^M m(i) \mathcal{B}(u_0, J_i) + \sum_{n=1}^N m(n) k_n^{2q+2} \int_{I_n} \|\partial_t^{q+1} u(t, \cdot)\|^2 dt + h^{2r+2} \sum_{n=0}^N \|u(t_n)\|_{r+1}^2 + \sum_{n=1}^N h^{2r+2} m(n) k_n \|u\|_{r+1, I_n}^2 \right)$$

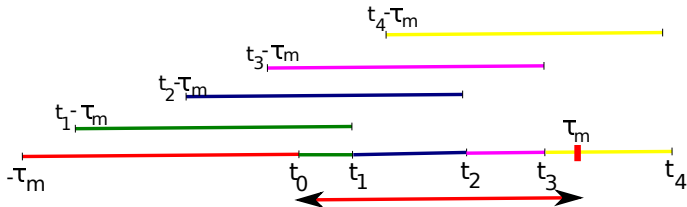
holds for $t_N \geq 0$, where C is a positive constant independent of the time step $k_n = t_n - t_{n-1}$ and the maximal space element diameter h .

Main difficulty: we cannot use the standard techniques for strongly parabolic PDEs

Best we can use: Grönwall's inequality

Proof of the error estimate

$$\begin{aligned} \eta(t_n) &\leq C_1 \eta(t_{n-1}) + C_2 \int_{t_{n-1}-\tau_{\max}}^{t_{n-1}} \eta(s) ds \\ &\quad + C_3 \int_{t_{n-1}-\tau_{\max}}^{t_n} \|\rho(s)\|^2 ds + C_4 \|\rho^{n-1}\|^2 + \frac{1}{\epsilon^2(1-\epsilon^2)} \|\rho^n\|^2, \end{aligned}$$



Main results:

- A new algorithm for the numerical solution of DDEs (NF)
- Error analysis
- Application to neural field models

Future work

- Spectral analysis in more space dimensions
- Extend the numerical model to more populations
- Computations in higher dimensions on arbitrary domain

Let $u \in C^1((0, T), \mathbb{R}) \cap C([0, T], \mathbb{R})$ be the solution of

$$\begin{aligned} \dot{u}(t) &= -\alpha u(t) + u(t - \tau), \quad t > 0, \\ u(s) &= u^0(s) = -s, \quad s \in [-\tau, 0], \end{aligned}$$

where $\alpha = 1$ and $\tau = 2$.

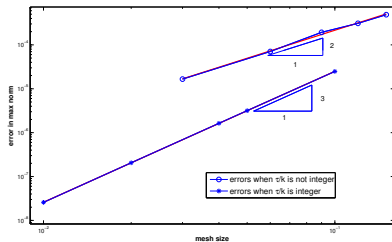
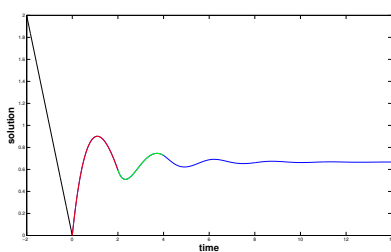


Figure 10: The dGcG(1) solution for $\alpha = 1$ (left). The accuracy of the method, on a log-log plot, (right) when τ/k is not an integer and when it is an integer.

Consider the integro-differential equation with source term g

$$\frac{\partial}{\partial t} u(t, x) + \alpha u(t, x) = \int_{\Omega} J(x, r) u(t, r) d r + g(t, x),$$

with $u(0, x) = u^0(x) = x$, $J(x, r) = 1$. When $g = 0$ and $\alpha = 1$, the exact solution is $u(x, t) = x e^{-t}$.

With this example we would like to demonstrate that the time accuracy is not destroyed when we add a spatial integral term.

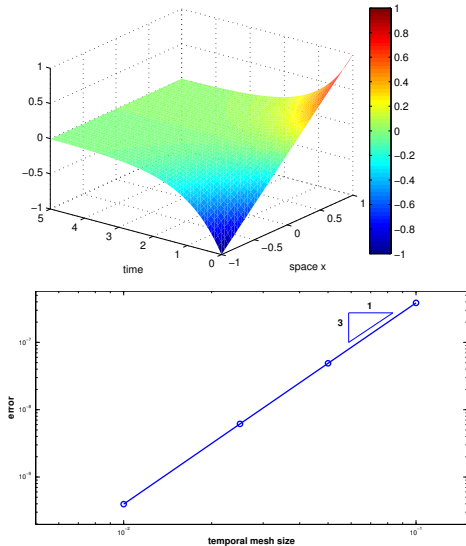


Figure 11: The dGcG(1) solution for $\alpha = 1$ and $g = 0$ (top). The accuracy of the method on a log-log plot (bottom).